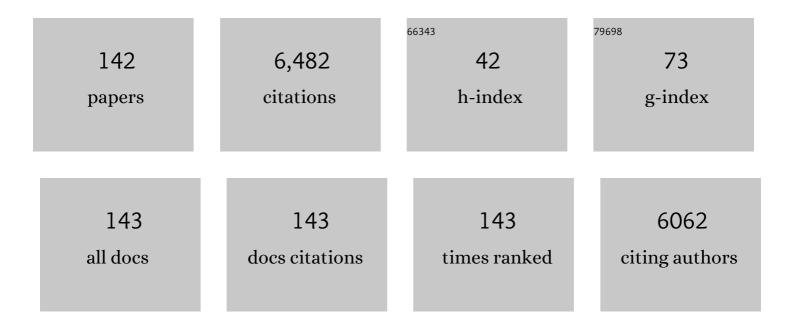
Xiangliang Pan

List of Publications by Year in descending order

Source: https://exaly.com/author-pdf/3751747/publications.pdf Version: 2024-02-01



#	Article	IF	CITATIONS
1	Effects of photo-irradiation on mercury binding to dissolved organic matter: Insights from FT-IR and synchronous fluorescence two-dimensional correlation spectroscopy. Chemosphere, 2022, 287, 132027.	8.2	18
2	Environmental behaviors of microplastics in aquatic systems: A systematic review on degradation, adsorption, toxicity and biofilm under aging conditions. Journal of Hazardous Materials, 2022, 423, 126915.	12.4	226
3	Accumulation of microplastics in tadpoles from different functional zones in Hangzhou Great Bay Area, China: Relation to growth stage and feeding habits. Journal of Hazardous Materials, 2022, 424, 127665.	12.4	14
4	Functional hydrogel for fast, precise and inhibition-free point-of-care bacteria analysis in crude food samples. Biomaterials, 2022, 280, 121278.	11.4	20
5	FT-IR and synchronous fluorescence two-dimensional correlation spectroscopic analysis on the binding properties of mercury onto humic acids as influenced by pH modification and sulfide addition. Science of the Total Environment, 2022, 819, 152047.	8.0	9
6	Insights into capture-inactivation/oxidation of antibiotic resistance bacteria and cell-free antibiotic resistance genes from waters using flexibly-functionalized microbubbles. Journal of Hazardous Materials, 2022, 428, 128249.	12.4	6
7	Response to the comments on "Environmental behaviors of microplastics in aquatic systems: A systematic review on degradation, adsorption, toxicity and biofilm under aging conditionsâ€: Journal of Hazardous Materials, 2022, 430, 128344.	12.4	3
8	<i>Sargassum horneri</i> â€based carbonâ€doped <scp>TiO₂</scp> and its aquatic naphthalene photodegradation under sunlight irradiation. Journal of Chemical Technology and Biotechnology, 2022, 97, 1267-1274.	3.2	3
9	Characteristics and distribution of microplastics in shoreline sediments of the Yangtze River, main tributaries and lakes in China—From upper reaches to the estuary. Environmental Science and Pollution Research, 2022, 29, 48453-48464.	5.3	8
10	Transport of mercury in a regulated high-sediment river and its input to marginal seas. Water Research, 2022, 214, 118211.	11.3	18
11	Binding of methylmercury to humic acids (HA): Influence of solar radiation and sulfide addition reaction of HA. Science of the Total Environment, 2022, 827, 154356.	8.0	8
12	Morphologically-different cells and colonies cause distinctive performance of coagulative colloidal ozone microbubbles in simultaneously removing bloom-forming cyanobacteria and microcystin-LR. Journal of Hazardous Materials, 2022, 435, 128986.	12.4	3
13	Fenton micro-reactor on a bubble: A novel microbubble-triggered simultaneous capture and catalytic oxidation strategy for recalcitrant organic pollutant removal. Science of the Total Environment, 2022, 835, 155556.	8.0	6
14	Chemical structure and nanomechanics relevant electrochemistry of solid-phase humic acid along a typical forest-river-paddy landscape section in eastern China and its environmental implications. Science of the Total Environment, 2022, 838, 156147.	8.0	3
15	One stone two birds: Bone char as a cost-effective material for stabilizing multiple heavy metals in soil and promoting crop growth. Science of the Total Environment, 2022, 840, 156163.	8.0	29
16	Transfer of Micro(nano)plastics in animals: A mini-review and future research recommendation. Journal of Hazardous Materials Advances, 2022, 7, 100101.	3.0	6
17	Passivation of heavy metals in copper–nickel tailings by in-situ bio-mineralization: A pilot trial and mechanistic analysis. Science of the Total Environment, 2022, 838, 156504.	8.0	15
18	Application of iron-based materials in heterogeneous advanced oxidation processes for wastewater treatment: A review. Chemical Engineering Journal, 2021, 407, 127191.	12.7	212

#	Article	IF	CITATIONS
19	Removal of micron-scale microplastic particles from different waters with efficient tool of surface-functionalized microbubbles. Journal of Hazardous Materials, 2021, 404, 124095.	12.4	60
20	Photocatalytic aging process of Nano-TiO2 coated polypropylene microplastics: Combining atomic force microscopy and infrared spectroscopy (AFM-IR) for nanoscale chemical characterization. Journal of Hazardous Materials, 2021, 404, 124159.	12.4	48
21	Mitigation of soil salinization and alkalization by bacterium-induced inhibition of evaporation and salt crystallization. Science of the Total Environment, 2021, 755, 142511.	8.0	29
22	Distinct fungal plastisphere across different river functional zones: A watershed scale study. Science of the Total Environment, 2021, 752, 141879.	8.0	18
23	An AFM-IR study on surface properties of nano-TiO2 coated polyethylene (PE) thin film as influenced by photocatalytic aging process. Science of the Total Environment, 2021, 757, 143900.	8.0	24
24	Microplastics generated under simulated fire scenarios: Characteristics, antimony leaching, and toxicity. Environmental Pollution, 2021, 269, 115905.	7.5	36
25	Potential of ozone micro-bombs in simultaneously fast removing bloom-forming cyanobacteria and in situ degrading microcystins. Chemical Engineering Journal, 2021, 407, 127186.	12.7	20
26	Effectively reducing antibiotic contamination and resistance in fishery by efficient gastrointestine-blood delivering dietary millispheres. Journal of Hazardous Materials, 2021, 409, 125012.	12.4	9
27	Nanoporous hydrogel for direct digital nucleic acid amplification in untreated complex matrices for single bacteria counting. Biosensors and Bioelectronics, 2021, 184, 113199.	10.1	27
28	Effects of advanced oxidation processes on leachates and properties of microplastics. Journal of Hazardous Materials, 2021, 413, 125342.	12.4	67
29	Abiotic mechanism changing tetracycline resistance in root mucus layer of floating plant: The role of antibiotic-exudate complexation. Journal of Hazardous Materials, 2021, 416, 125728.	12.4	2
30	Fe(III) greatly promotes peroxymonosulfate activation by WS2 for efficient carbamazepine degradation and Escherichia coli disinfection. Science of the Total Environment, 2021, 787, 147724.	8.0	34
31	Long-term effects of four environment-related iron minerals on microbial anaerobic oxidation of methane in paddy soil: A previously overlooked role of widespread goethite. Soil Biology and Biochemistry, 2021, 161, 108387.	8.8	15
32	Activation of peroxymonosulfate by iron oxychloride with hydroxylamine for ciprofloxacin degradation and bacterial disinfection. Science of the Total Environment, 2021, 799, 149506.	8.0	30
33	Synergistic activation of peroxymonosulfate and persulfate by ferrous ion and molybdenum disulfide for pollutant degradation: Theoretical and experimental studies. Chemosphere, 2020, 240, 124979.	8.2	72
34	Impact of salinity on colloidal ozone aphrons in removing phenanthrene from sediments. Journal of Hazardous Materials, 2020, 384, 121436.	12.4	11
35	Simultaneous removal of As(III) and Cu(II) from real bottom ash leachates by manganese-oxidizing aerobic granular sludge: Performance and mechanisms. Science of the Total Environment, 2020, 700, 134510.	8.0	18
36	Effective stabilization of arsenic in contaminated soils with biogenic manganese oxide (BMO) materials. Environmental Pollution, 2020, 258, 113481.	7.5	54

#	Article	IF	CITATIONS
37	Effects of accelerated aging on characteristics, leaching, and toxicity of commercial lead chromate pigmented microplastics. Environmental Pollution, 2020, 257, 113475.	7.5	136
38	Selectively enrichment of antibiotics and ARGs by microplastics in river, estuary and marine waters. Science of the Total Environment, 2020, 708, 134594.	8.0	133
39	Recent advances in municipal landfill leachate: A review focusing on its characteristics, treatment, and toxicity assessment. Science of the Total Environment, 2020, 703, 135468.	8.0	319
40	Insights into the transcriptional responses of a microbial community to silver nanoparticles in a freshwater microcosm. Environmental Pollution, 2020, 258, 113727.	7.5	36
41	Complex effects of pH and organic shocks on arsenic oxidation and removal by manganese-oxidizing aerobic granular sludge in sequencing batch reactors. Chemosphere, 2020, 260, 127621.	8.2	7
42	Microplastics in agricultural soils: Extraction and characterization after different periods of polythene film mulching in an arid region. Science of the Total Environment, 2020, 749, 141420.	8.0	120
43	Inhibitory effects of polystyrene microplastics on caudal fin regeneration in zebrafish larvae. Environmental Pollution, 2020, 266, 114664.	7.5	25
44	Nanoscale infrared, thermal and mechanical properties of aged microplastics revealed by an atomic force microscopy coupled with infrared spectroscopy (AFM-IR) technique. Science of the Total Environment, 2020, 744, 140944.	8.0	46
45	Rapid removal of organic micropollutants by heterogeneous peroxymonosulfate catalysis over a wide pH range: Performance, mechanism and economic analysis. Separation and Purification Technology, 2020, 248, 117023.	7.9	36
46	Weathering alters surface characteristic of TiO2-pigmented microplastics and particle size distribution of TiO2 released into water. Science of the Total Environment, 2020, 729, 139083.	8.0	45
47	Enhanced decomposition of H2O2 by molybdenum disulfide in a Fenton-like process for abatement of organic micropollutants. Science of the Total Environment, 2020, 732, 139335.	8.0	56
48	Increased inheritance of structure and function of bacterial communities and pathogen propagation in plastisphere along a river with increasing antibiotics pollution gradient. Environmental Pollution, 2020, 265, 114641.	7.5	49
49	Applications of nanozymes in the environment. Environmental Science: Nano, 2020, 7, 1305-1318.	4.3	87
50	Photochemical behaviors of mercury (Hg) species in aquatic systems: A systematic review on reaction process, mechanism, and influencing factor. Science of the Total Environment, 2020, 720, 137540.	8.0	50
51	Enantioselective effects of imazethapyr on Arabidopsis thaliana root exudates and rhizosphere microbes. Science of the Total Environment, 2020, 716, 137121.	8.0	37
52	What occurs in colloidal gas aphron-induced separation of titanium dioxide nanoparticles? Particle fate analysis by tracking technologies. Science of the Total Environment, 2020, 716, 137104.	8.0	8
53	Lability-specific enrichment of typical engineered metal (oxide) nanoparticles by surface-functionalized microbubbles from waters. Science of the Total Environment, 2020, 719, 137526.	8.0	5
54	Aging of microplastics affects their surface properties, thermal decomposition, additives leaching and interactions in simulated fluids. Science of the Total Environment, 2020, 714, 136862.	8.0	190

#	Article	IF	CITATIONS
55	Enantioselective effects of imazethapyr residues on Arabidopsis thaliana metabolic profile and phyllosphere microbial communities. Journal of Environmental Sciences, 2020, 93, 57-65.	6.1	23
56	Enhanced performance of tetracycline treatment in wastewater using aerobic granular sludge with in-situ generated biogenic manganese oxides. Science of the Total Environment, 2020, 735, 139533.	8.0	31
57	Transport and retention of biogenic selenium nanoparticles in biofilm-coated quartz sand porous media and consequence for elemental mercury immobilization. Science of the Total Environment, 2019, 692, 1116-1124.	8.0	16
58	Comparison of coagulative colloidal microbubbles with monomeric and polymeric inorganic coagulants for tertiary treatment of distillery wastewater. Science of the Total Environment, 2019, 694, 133649.	8.0	14
59	Metal oxyanion removal from wastewater using manganese-oxidizing aerobic granular sludge. Chemosphere, 2019, 236, 124353.	8.2	25
60	Cultivation of a versatile manganese-oxidizing aerobic granular sludge for removal of organic micropollutants from wastewater. Science of the Total Environment, 2019, 690, 417-425.	8.0	16
61	Methane emissions from aqueous sediments are influenced by complex interactions among microbes and environmental factors: A modeling study. Water Research, 2019, 166, 115086.	11.3	6
62	Suppression of coal dust by microbially induced carbonate precipitation usingStaphylococcus succinus. Environmental Science and Pollution Research, 2019, 26, 35968-35977.	5.3	30
63	Detection of engineered nanoparticles in aquatic environments: current status and challenges in enrichment, separation, and analysis. Environmental Science: Nano, 2019, 6, 709-735.	4.3	81
64	Ozone-encapsulated colloidal gas aphrons for in situ and targeting remediation of phenanthrene-contaminated sediment-aquifer. Water Research, 2019, 160, 29-38.	11.3	26
65	Efficient elimination and re-growth inhibition of harmful bloom-forming cyanobacteria using surface-functionalized microbubbles. Water Research, 2019, 161, 473-485.	11.3	22
66	Leaching behavior of fluorescent additives from microplastics and the toxicity of leachate to Chlorella vulgaris. Science of the Total Environment, 2019, 678, 1-9.	8.0	188
67	Effects of imazethapyr spraying on plant growth and leaf surface microbial communities in Arabidopsis thaliana. Journal of Environmental Sciences, 2019, 85, 35-45.	6.1	20
68	The kinetics, thermodynamics and mineral crystallography of CaCO3 precipitation by dissolved organic matter and salinity. Science of the Total Environment, 2019, 673, 546-552.	8.0	17
69	Hydroxylamine-facilitated degradation of rhodamine B (RhB) and p-nitrophenol (PNP) as catalyzed by Fe@Fe2O3 core-shell nanowires. Journal of Molecular Liquids, 2019, 282, 13-22.	4.9	38
70	Immobilization of elemental mercury by biogenic Se nanoparticles in soils of varying salinity. Science of the Total Environment, 2019, 668, 303-309.	8.0	16
71	Multiple-pathway arsenic oxidation and removal from wastewater by a novel manganese-oxidizing aerobic granular sludge. Water Research, 2019, 157, 83-93.	11.3	56
72	Ca2+ complexation of dissolved organic matter in arid inland lakes is significantly affected by drastic seasonal change of salinity. Science of the Total Environment, 2019, 663, 479-485.	8.0	12

#	Article	IF	CITATIONS
73	Removal of bacteriophage f2 in water by Fe/Ni nanoparticles: Optimization of Fe/Ni ratio and influencing factors. Science of the Total Environment, 2019, 649, 995-1003.	8.0	19
74	Soil dissolved organic matter affects mercury immobilization by biogenic selenium nanoparticles. Science of the Total Environment, 2019, 658, 8-15.	8.0	22
75	Fabricating biogenic Fe(III) flocs from municipal sewage sludge using NAFO processes: Characterization and arsenic removal ability. Journal of Environmental Management, 2019, 231, 268-274.	7.8	16
76	Heteroaggregation of soil particulate organic matter and biogenic selenium nanoparticles for remediation of elemental mercury contamination. Chemosphere, 2019, 221, 486-492.	8.2	18
77	Simultaneous remediation of As(III) and dibutyl phthalate (DBP) in soil by a manganese-oxidizing bacterium and its mechanisms. Chemosphere, 2019, 220, 837-844.	8.2	30
78	Effects of 17α‑ethinylestradiol on caudal fin regeneration in zebrafish larvae. Science of the Total Environment, 2019, 653, 10-22.	8.0	16
79	Effects of different concentrations of Microcystis aeruginosa on the intestinal microbiota and immunity of zebrafish (Danio rerio). Chemosphere, 2019, 214, 579-586.	8.2	36
80	Responses of unicellular alga Chlorella pyrenoidosa to allelochemical linoleic acid. Science of the Total Environment, 2018, 625, 1415-1422.	8.0	46
81	A survey of uranium levels in urine and hair of people living in a coal mining area in Yili, Xinjiang, China. Journal of Environmental Radioactivity, 2018, 189, 168-174.	1.7	28
82	Differences in Sb(V) and As(V) adsorption onto a poorly crystalline phyllomanganate (δ-MnO2): Adsorption kinetics, isotherms, and mechanisms. Chemical Engineering Research and Design, 2018, 113, 40-47.	5.6	56
83	Interactions between biogenic selenium nanoparticles and goethite colloids and consequence for remediation of elemental mercury contaminated groundwater. Science of the Total Environment, 2018, 613-614, 672-678.	8.0	35
84	Multiple-pathway remediation of mercury contamination by a versatile selenite-reducing bacterium. Science of the Total Environment, 2018, 615, 615-623.	8.0	33
85	Microbiological and environmental significance of metal-dependent anaerobic oxidation of methane. Science of the Total Environment, 2018, 610-611, 759-768.	8.0	96
86	Stabilizing interaction of exopolymers with nano-Se and impact on mercury immobilization in soil and groundwater. Environmental Science: Nano, 2018, 5, 456-466.	4.3	22
87	Oxygenic denitrification for nitrogen removal with less greenhouse gas emissions: Microbiology and potential applications. Science of the Total Environment, 2018, 621, 453-464.	8.0	28
88	The combined toxicity effect of nanoplastics and glyphosate on Microcystis aeruginosa growth. Environmental Pollution, 2018, 243, 1106-1112.	7.5	202
89	Optimization of methane-dependent oxygenic denitrification in sequencing batch reactors by insights into the microbial interactions. Science of the Total Environment, 2018, 643, 623-631.	8.0	4
90	Adsorption capacities of poorly crystalline Fe minerals for antimonate and arsenate removal from water: adsorption properties and effects of environmental and chemical conditions. Clean Technologies and Environmental Policy, 2018, 20, 2169-2179.	4.1	12

#	Article	IF	CITATIONS
91	Bio-transformation and stabilization of arsenic (As) in contaminated soil using arsenic oxidizing bacteria and FeCl3 amendment. 3 Biotech, 2017, 7, 50.	2.2	15
92	Effect of Nitrite on the Formation of Trichloronitromethane (TCNM) During Chlorination of Polyhydroxy-Phenols and Sugars. Water, Air, and Soil Pollution, 2017, 228, 1.	2.4	5
93	Aerobic and anaerobic biosynthesis of nano-selenium for remediation of mercury contaminated soil. Chemosphere, 2017, 170, 266-273.	8.2	98
94	Photo-flocculation of microbial mat extracellular polymeric substances and their transformation into transparent exopolymer particles: Chemical and spectroscopic evidences. Scientific Reports, 2017, 7, 9074.	3.3	31
95	Spatial Variability of Cyanobacteria and Heterotrophic Bacteria in Lake Taihu (China). Bulletin of Environmental Contamination and Toxicology, 2017, 99, 380-384.	2.7	35
96	A microscopic and spectroscopic study of rapid antimonite sequestration by a poorly crystalline phyllomanganate: differences from passivated arsenite oxidation. RSC Advances, 2017, 7, 38377-38386.	3.6	21
97	Uranium Bioreduction and Biomineralization. Advances in Applied Microbiology, 2017, 101, 137-168.	2.4	42
98	Microbially-induced Carbonate Precipitation for Immobilization of Toxic Metals. Advances in Applied Microbiology, 2016, 94, 79-108.	2.4	143
99	Role of <i>Acinetobacter</i> sp. in arsenite As(III) oxidation and reducing its mobility in soil. Chemistry and Ecology, 2016, 32, 460-471.	1.6	16
100	Bioremediation of Nitrate- and Arsenic-Contaminated Groundwater Using Nitrate-Dependent Fe(II) Oxidizing <i>Clostridium</i> sp. Strain pxl2. Geomicrobiology Journal, 2016, 33, 185-193.	2.0	30
101	Effects of pH and Salinity on Adsorption of Hypersaline Photosynthetic Microbial Mat Exopolymers to Goethite: A Study Using a Quartz Crystal Microbalance and Fluorescence Spectroscopy. Geomicrobiology Journal, 2016, 33, 332-337.	2.0	5
102	Biostabilization of Desert Sands Using Bacterially Induced Calcite Precipitation. Geomicrobiology Journal, 2016, 33, 243-249.	2.0	30
103	Bioimmobilization of Heavy Metals in Acidic Copper Mine Tailings Soil. Geomicrobiology Journal, 2016, 33, 261-266.	2.0	66
104	Biomineralization, Bioremediation and Biorecovery of Toxic Metals and Radionuclides. Geomicrobiology Journal, 2016, 33, 175-178.	2.0	34
105	Effects of pH Shock on Hg(II) Complexation by Exopolymers from <i>Acidithiobacillus ferrooxidans</i> . Geomicrobiology Journal, 2016, 33, 325-331.	2.0	5
106	Multiple metal-resistant bacteria and fungi from acidic copper mine tailings of Xinjiang, China. Environmental Earth Sciences, 2015, 74, 3113-3121.	2.7	31
107	Effect of exopolymers on oxidative dissolution of natural rhodochrosite by Pseudomonas putida strain MnB1: An electrochemical study. Applied Geochemistry, 2015, 59, 95-103.	3.0	6
108	Influence of ofloxacin on photosystems I and II activities of Microcystis aeruginosa and the potential role of cyclic electron flow. Journal of Bioscience and Bioengineering, 2015, 119, 159-164.	2.2	37

#	Article	IF	CITATIONS
109	Effects of salinity and (an)ions on arsenic behavior in sediment of Bosten Lake, Northwest China. Environmental Earth Sciences, 2015, 73, 4707-4716.	2.7	17
110	Simultaneous removal of tetracycline hydrochloride and As(III) using poorly-crystalline manganese dioxide. Chemosphere, 2015, 136, 102-110.	8.2	54
111	Effects of irradiation and pH on fluorescence properties and flocculation of extracellular polymeric substances from the cyanobacterium Chroococcus minutus. Colloids and Surfaces B: Biointerfaces, 2015, 128, 115-118.	5.0	24
112	Bioreduction of Hexavalent Chromium from Soil Column Leachate by <i>Pseudomonas stutzeri</i> . Bioremediation Journal, 2015, 19, 249-258.	2.0	11
113	Analysis of the Proteome of the Marine Diatom <i>Phaeodactylum tricornutum</i> Exposed to Aluminum Providing Insights into Aluminum Toxicity Mechanisms. Environmental Science & Technology, 2015, 49, 11182-11190.	10.0	40
114	Extracellular polymeric substances buffer against the biocidal effect of H2O2 on the bloom-forming cyanobacterium Microcystis aeruginosa. Water Research, 2015, 69, 51-58.	11.3	108
115	Anaerobic Nitrate-Dependent Iron (II) Oxidation by a Novel Autotrophic Bacterium, <i>Citrobacter freundii</i> Strain PXL1. Geomicrobiology Journal, 2014, 31, 138-144.	2.0	59
116	Interaction of dissolved organic matter with Hg(II) along salinity gradient in Boston Lake. Geochemistry International, 2014, 52, 1072-1077.	0.7	8
117	Continuous volatile fatty acid production from waste activated sludge hydrolyzed at pH 12. Bioresource Technology, 2014, 168, 173-179.	9.6	42
118	Biosorption of Hg(II) onto goethite with extracellular polymeric substances. Bioresource Technology, 2014, 160, 119-122.	9.6	19
119	Aerobic granulation of aggregating consortium X9 isolated from aerobic granules and role of cyclic di-GMP. Bioresource Technology, 2014, 152, 557-561.	9.6	44
120	Herbicidal effects of harmaline from Peganum harmala on photosynthesis of Chlorella pyrenoidosa: Probed by chlorophyll fluorescence and thermoluminescence. Pesticide Biochemistry and Physiology, 2014, 115, 23-31.	3.6	12
121	Microscopic morphology and elemental composition of size distributed atmospheric particulate matter in Urumqi, China. Environmental Earth Sciences, 2013, 69, 2139-2150.	2.7	16
122	A system dynamics approach for water resources policy analysis in arid land: a model for Manas River Basin. Journal of Arid Land, 2013, 5, 118-131.	2.3	34
123	A Dynamic Model for Vulnerability Assessment of Regional Water Resources in Arid Areas: A Case Study of Bayingolin, China. Water Resources Management, 2013, 27, 3085-3101.	3.9	120
124	Removal of antimony (Sb(V)) from Sb mine drainage: Biological sulfate reduction and sulfide oxidation–precipitation. Bioresource Technology, 2013, 146, 799-802.	9.6	92
125	Disintegration of aerobic granules: Role of second messenger cyclic di-GMP. Bioresource Technology, 2013, 146, 330-335.	9.6	97
126	Root exudates from sunflower (<i>Helianthus annuus</i> L.) show a strong adsorption ability toward Cd(II). Journal of Plant Interactions, 2013, 8, 263-270.	2.1	18

#	Article	IF	CITATIONS
127	Lead Complexation of Soluble and Bound Extracellular Polymeric Substances from Activated Sludge: Characterized with Fluorescence Spectroscopy and Ftir Spectroscopy. Biotechnology and Biotechnological Equipment, 2012, 26, 3371-3377.	1.3	11
128	Lead complexation behaviour of root exudates of salt marsh plant <i>Salicornia europaea</i> L. Chemical Speciation and Bioavailability, 2012, 24, 60-63.	2.0	15
129	Effects of heat treatment on fluorescence properties of humic substances from sandy soil in arid land and their Hg(II) binding behaviors. Environmental Earth Sciences, 2012, 66, 2273-2279.	2.7	9
130	Biosorption of Cu(II) to extracellular polymeric substances (EPS) from Synechoeystis sp.: a fluorescence quenching study. Frontiers of Environmental Science and Engineering, 2012, 6, 493-497.	6.0	20
131	Effects of Sb(V) on Growth and Chlorophyll Fluorescence of Microcystis aeruginosa (FACHB-905). Current Microbiology, 2012, 65, 733-741.	2.2	11
132	Biomineralization based remediation of As(III) contaminated soil by Sporosarcina ginsengisoli. Journal of Hazardous Materials, 2012, 201-202, 178-184.	12.4	282
133	Cu(II) complexation of high molecular weight (HMW) fluorescent substances in root exudates from a wetland halophyte (Salicornia europaea L.). Journal of Bioscience and Bioengineering, 2011, 111, 193-197.	2.2	18
134	Antimony Accumulation, Growth Performance, Antioxidant Defense System and Photosynthesis of Zea mays in Response to Antimony Pollution in Soil. Water, Air, and Soil Pollution, 2011, 215, 517-523.	2.4	86
135	Remediation of copper-contaminated soil by Kocuria flava CR1, based on microbially induced calcite precipitation. Ecological Engineering, 2011, 37, 1601-1605.	3.6	206
136	Earthworms (Eisenia foetida, Savigny) mucus as complexing ligand for imidacloprid. Biology and Fertility of Soils, 2010, 46, 845-850.	4.3	32
137	Toxic effects of antimony on photosystem II of Synechocystis sp. as probed by in vivo chlorophyll fluorescence. Journal of Applied Phycology, 2010, 22, 479-488.	2.8	70
138	Binding of dicamba to soluble and bound extracellular polymeric substances (EPS) from aerobic activated sludge: A fluorescence quenching study. Journal of Colloid and Interface Science, 2010, 345, 442-447.	9.4	86
139	Binding of phenanthrene to extracellular polymeric substances (EPS) from aerobic activated sludge: A fluorescence study. Colloids and Surfaces B: Biointerfaces, 2010, 80, 103-106.	5.0	80
140	EFFECT OF CHROMIUM(VI) ON PHOTOSYSTEM II ACTIVITY AND HETEROGENEITY OF <i>SYNECHOCYSTIS</i> SP. (CYANOPHYTA): STUDIED WITH IN VIVO CHLOROPHYLL FLUORESCENCE TESTS ¹ . Journal of Phycology, 2009, 45, 386-394.	2.3	17
141	Effects of levofloxacin hydrochlordie on photosystem II activity and heterogeneity of Synechocystis sp Chemosphere, 2009, 77, 413-418.	8.2	41
142	Toxic effects of amoxicillin on the photosystem II of Synechocystis sp. characterized by a variety of in vivo chlorophyll fluorescence tests. Aquatic Toxicology, 2008, 89, 207-213.	4.0	110